Increases in Calmodulin Abundance and Stabilization of Activated Inducible Nitric Oxide Synthase Mediate Bacterial Killing in RAW 264.7 Macrophages †

ARTICLE *in* BIOCHEMISTRY · SEPTEMBER 2006

Impact Factor: 3.02 · DOI: 10.1021/bi060485p · Source: PubMed

3 AUTHORS, INCLUDING:

Heather S Smallwood

The University of Tennessee Health Science …

20 PUBLICATIONS **446** CITATIONS

SEE PROFILE

Increases in Calmodulin Abundance and Stabilization of Activated Inducible Nitric Oxide Synthase Mediate Bacterial Killing in RAW 264.7 Macrophages†

Heather S. Smallwood, Liang Shi, and Thomas C. Squier*

Biological Sciences Division, Pacific Northwest National Laboratory, Richland, Washington 99354

Received March 10, 2006; Revised Manuscript Received June 13, 2006

ABSTRACT: The rapid activation of macrophages in response to bacterial antigens is central to the innate immune system that permits the recognition and killing of pathogens to limit infection. To understand regulatory mechanisms underlying macrophage activation, we have investigated changes in the abundance of calmodulin (CaM) and iNOS in response to the bacterial cell wall component lipopolysaccharide (LPS) using RAW 264.7 macrophages. Critical to these measurements was the ability to differentiate free iNOS from the CaM-bound (active) form of iNOS associated with nitric oxide generation. We observe a rapid 2-fold increase in CaM abundance during the first 30 min that is blocked by inhibition of either NFκB nuclear translocation or protein synthesis. A similar 2-fold increase in the abundance of the complex between CaM and iNOS is observed with the same time dependence. In contrast, there are no detectable increases in the CaM-free (i.e., inactive) form of iNOS within the first 2 h; it remains at a very low abundance during the initial phase of macrophage activation. Increasing cellular CaM levels in stably transfected macrophages results in a corresponding increase in the abundance of the CaM/iNOS complex that promotes effective bacterial killing following infection by *Salmonella typhimurium*. Thus, LPS-dependent increases in CaM abundance function in the stabilization and activation of iNOS on the rapid time scale associated with macrophage activation and bacterial killing. These results explain how CaM and iNOS coordinately function to form a stable complex that is part of a rapid host response that functions within the first 30 min following bacterial infection to upregulate the innate immune system involving macrophage activation.

Age-related declines in immune function and associated increases in the inflammatory response in surrounding tissues may be the result of aberrant mechanisms of macrophage activation, which have the potential to contribute to observed changes in the abundance of circulating inflammatory cytokines (*1*−*4*). Macrophages are primary lines of defense that underlie the innate immune system, whereby bacterial and viral threats are detected and eliminated through (i) phagocytosis and the coordinated generation of reactive oxygen and nitrogen species and (ii) paracrine signaling through the release of inflammatory cytokines (*5*−*7*). Mechanistically, macrophage activation and the resultant oxidative burst necessary for bacterial killing have been suggested to require the coordinate upregulation of key enzymes, including NADPH oxidase, cyclooxygenase 2, and inducible nitric oxide synthase (iNOS),[1] that are associated respectively with the generation of superoxide, prostaglandins, and nitric oxide to potentiate cellular activation and generate highly reactive and long-lived nitrative species (e.g., NO_2^-, NO_3^-, and $ONOO^-$) associated with pathogen killing (*8*−*13*). CaM binding to iNOS is necessary for activation and functions to coordinate calcium-dependent signaling and iNOS activation with autocrine pathways involving inflammatory cytokines (e.g., TNFα) to modulate macrophage activation (*4*). Thus, iNOS expression is regulated by cytokine-dependent activation of critical signaling pathways. At the same time, pathogen-dependent increases in CaM abundance are necessary for iNOS activity and the modulation of apoptotic responses (*4*). Furthermore, defective activation of CaM-dependent pathways contributes to the ability of *Mycobacterium tuberculosis* to parasitize macrophages (*14*), suggesting a key role for CaM in modulating macrophage activation. Thus, observed age-dependent declines in CaM function and abundance may relate to observed declines in immune function (*2*, *15*−*20*). However, the downregulation of CaM function through the addition of inhibitors and binding peptides can also activate macrophages and block bacterial infections (*21*, *22*), suggesting a multi-

† This work was supported by grants from the National Institutes of Health (NIA AG12993 and AG17996) and by the Laboratory Directed Research and Development Program of the Pacific Northwest National Laboratory, operated for the U.S. Department of Energy by Battelle Memorial Institute.

* To whom correspondence should be addressed. Tel: (509) 376-2218. Fax: (509) 376-6767. E-mail: thomas.squier@pnl.gov.

[1] Abbreviations: CaM, calmodulin; EGTA, ethylene glycol bis(β-aminoethyl ether)-*N*,*N*,*N*′,*N*′-tetraacetic acid; FBS, fetal bovine serum; HRP, horseradish peroxidase; IκB, inhibitor of NFκB; IκBαM, dominant-negative mutant of IκB in which phosphorylation sites for IκB kinase are mutated (i.e., S32A and S36A); IFNγ, interferon γ; IRF, interferon regulatory factor; iNOS, inducible nitric oxide synthase; LB, Luria−Bertani broth; LPS, lipopolysaccharide; MEF, myocyte enhancer factor; NFκB, nuclear factor κ B; Nramp1, natural resistance-associated macrophage protein 1; PBS, phosphate-buffered saline; RAW^{CaM}, RAW 264.7 macrophages transfected with DNA encoding CaM; RAW^{Nramp1}, RAW 264.7 macrophages transfected with DNA encoding the divalent cation transporter Nramp1; ROS, reactive oxygen species; RNS, reactive nitrogen species; SDS−PAGE, sodium dodecyl sulfate−polyacrylamide gel electrophoresis; Sp1, specificity protein 1; TNFα, tumor necrosis factor α.

10.1021/bi060485p CCC: $33.50
Published on Web 07/25/2006

factorial role for CaM in mediating macrophage activation and bacterial killing.

CaM is known to associate and modulate the function of more than 50 target proteins, functioning as a central regulator of metabolism in all cells, including macrophages where CaM association with iNOS is necessary for enzyme function and stabilization (*23*−*28*). The generation of NO$^{\bullet}$ by iNOS has been suggested to contribute to the generation of reactive nitrogen species and associated antibacterial activity (*29*). A comparison of macrophage killing following exposure of peritoneal macrophages isolated from wild-type or iNOS knock-out animals to *Salmonella typhimurium* suggested an important early role for iNOS in mediating bacterial killing (*30*). However, the kinetics of changes in iNOS abundance in response to exposure to bacterial antigens has been reported to occur on a time scale of several hours and is slow in comparison with the known kinetics of the oxidative burst, the generation of reactive nitrogen species, and the initial host response associated with bacterial killing (*29*−*31*). Indeed, iNOS protein is typically not detected until 4 h after exposure to the bacterial antigen LPS, suggesting that iNOS may function primarily as part of a bacteriostatic mechanism for long times following infection and that other enzymes may contribute to the formation of nitrating species detected by the Griess reaction (*4*, *31*−*34*). In fact, following exposure to *S. typhimurium* the vast majority of internalized bacteria are killed within 2 h, before increases in iNOS protein abundance are typically detected using Western immunoblots (*29*−*31*). For these reasons, the precise role of iNOS in mediating the antibacterial action associated with the macrophage response has remained uncertain.

To better understand the cellular regulation of iNOS and its relationship to the antibacterial activity of macrophages, we have investigated time-dependent changes in the abundance of iNOS and its activator protein CaM in response to exposing macrophages to the bacterial endotoxin LPS. Critical to these measurements was the ability to separately resolve uncomplexed and inactive iNOS from the CaM-bound complex with iNOS that is functionally active. In response to LPS exposure, there is a rapid 2-fold increase in the abundance of CaM and its functional complex with iNOS (i.e., CaM/iNOS) that occurs within the first 30 min. In contrast, the uncomplexed form of iNOS is present at a low and constant level during the first 2 h. LPS-dependent increases in CaM abundance and binding to iNOS stabilize the activated form of the CaM/iNOS enzyme complex and prevent the rapid degradation of iNOS by endogenous proteases. This stabilized CaM/iNOS complex results in upregulation of bactericidal activity of macrophages to rapidly eliminate internalized *S. typhimurium*. These results suggest an important and previously unrecognized role for CaM as a central regulator in mediating macrophage activation.

EXPERIMENTAL PROCEDURES

Materials. Actinomycin D, cyclohexamide, lactacystin, sulfasalazine, and bacterial LPS from *Escherichia coli* strain O127:B8 were purchased from Sigma Chemical Co. (St. Louis, MO). Interferon γ was from Santa Cruz Biotechnology, Inc. (Santa Cruz, CA). Ampicillin, RPMI 1640 medium (no.0030078DJ), fetal bovine serum (FBS), penicillin, streptomycin, and G418 were from Gibco (Carlsbad, CA). FuGENE 6 transfection reagent was from Roche (Indianapolis, IN). A vector set containing a dominant-negative IκBα (i.e., IκBαM) was from BD Biosciences (Palo Alto, CA). Purified iNOS was obtained from Cayman Chemical Co. (Ann Arbor, MI). Antibodies used include a monoclonal antibody against glyceraldehyde-3-phosphate dehydrogenase (GAPDH) (AbCaM, Cambridge, MA), a polyclonal antibody against full-length CaM (sc-5537; Santa Cruz Biotechnology, Inc.), and six distinct polyclonal antibodies against synthetic peptides derived from the murine iNOS sequence. Antibodies tested against iNOS include M19 (sc-650) and C11 (sc-7271) against C-terminal peptides and N20 (sc-651) and H174 (sc-8310) against N-terminal peptides (Santa Cruz Biotechnology, Inc.), C-terminal amino acids (CKKGSALEERKATRL^{1144}) (catalog no. 482729; Calbiochem), and a C-terminal fragment 961−1144 (catalog no. 610332; BD Biosciences). Antibody sc-650 was used in all measurements of iNOS abundance in cellular lysates, since this antibody provided optimal resolution of both the full-length protein and large fragments whose abundance were affected by macrophage activation. However, all antibodies permitted detection of full-length purified iNOS uncomplexed with CaM on Western blots, with the following sensitivities: sc-650 > H174 > sc-651 > sc-7271. Antibodies from Calbiochem and BD Transduction Laboratories displayed very high backgrounds and were not useful for immunoblots against cellular lysates. Wild-type RAW 264.7 murine macrophages and a mutant overexpressing the natural resistance-associated macrophage protein 1 (Nramp1) were respectively obtained from Drs. Brian D. Thrall and Philippe Gros, where the Nramp1 construct was previously described in full (*35*).

Cell Culture Procedures. RAW 264.7 macrophages were grown to ~70% confluency in RPMI 1640 medium supplemented with 10% heat-inactivated FBS and a 1% mixture of penicillin and ampicillin (both at 1% v/v) in a humidified atmosphere of 5% CO_2 and 95% air at 37 °C, where total cell passages were kept below 80 for all experiments. Treatments involved the bacterial antigen LPS (10 ng/mL) for indicated times and, when indicated, prior incubation with one of the following inhibitors for the indicated times: actinomycin D (5 μM for 90 min), cycloheximide (100 μg/mL for 10 min), lactacystin (1 μM for 30 min), or sulfasalazine (2 mM for 30 min). Media were removed from each plate and pooled into a sterile flask before adding the appropriate amount of reagent and returning them to the plates for the indicated times. Prior to harvesting the cells, the medium was aspirated, and the cell monolayer was gently but thoroughly rinsed once with chilled D-PBS (Invitrogen, Carlsbad, CA) to remove residual serum and LPS. Then cells were placed on ice, and chilled lysis buffer [20 mM Tris (pH 8.0), 1% Nonidet P-40, 0.15 M NaCl, 1 mM Na_2PO_4, and 1 mM EGTA] was applied to the cell monolayer. The cells were then manually removed with cell lifters, and the lysate was placed directly into a chilled glass homogenizer to be kept on ice for the remainder of the procedure. A ten-stroke homogenization was applied to each sample, which was then immediately centrifuged for 15−30 min at 13000 rpm at 4 °C. The supernatant was removed, processed, and subjected to immunoblotting with the remainder of the sample stored at −80 °C pending further analysis.

CaM Expression and Purification. Complementary DNA corresponding to the coding region for chicken CaM [accession number MCCH (PIR database) or P02593 (SWISS-PROT database)] subcloned into pET-15b and transformed into the *E. coli* BL21 (DE3) cell strain was used for protein overexpression. The bacteria were grown in Lysogeny broth (LB or Luria−Bertani broth), and protein production was induced with isopropyl β-D-1-thiogalactopyranoside (IPTG). The CaM was purified by chromatography on phenyl-Sepharose CL-4B, essentially as previously described (*36*, *37*).

RAW 264.7 Transfection. The gene encoding CaM was subcloned into the a pcDNA3.1 vector (Invitrogen) that is designed to maintain a high level of stable expression in mammalian hosts, essentially as previously described (*4*). Vector amplification involved the transformation of *E. coli* and plasmid purification using a plasmid midi kit (Qiagen, Valencia, CA). RAW 264.7 macrophages were transfected with either pcDNA3.1 ± CaM gene or pCMV ± IκBαM using the Fugene transfection reagent (Roche, Indianapolis, IN), where IκBαM is a dominant-negative construct of IκB obtained from BD Bioscience (catalog no. K6012-1; Palo Alto, CA) whose phosphorylation sites for IκB kinase were mutated (i.e., S32A, S36A). Stable transfectants were maintained in RPMI media supplemented with G418 as the selection agent.

NO Measurement. The activity of iNOS was determined by measuring the release of the stable nitrite end product using Griess reagent (Pierce Inc., Rockford, IL) and monitoring absorbance at 560 nm using a microtiter plate reader at a 24 h time point. Prior to measurement, all nitrate was enzymatically converted to nitrite using nitrate reductase. Nitrite concentrations in conditioned media were determined on the basis of standard curves calibrated using sodium nitrite as a standard, as previously described (*4*).

Western Blot Analysis. Protein concentrations of cellular lysates were determined by the Coomassie Plus Bradford reagent from Pierce (Rockland, IL) immediately after harvesting cells. Aliquots of equal protein were reduced with NuPAGE reducing agent, diluted into NuPAGE LDS sample buffer, and denatured by boiling for 5 min prior to the separation of proteins by SDS−polyacrylamide gel electrophoresis on a 4−12% NuPAGE Bis-Tris gel, where all reagents were from Invitrogen (Carlsbad, CA). After electroblotting onto 0.45 μm nitrocellulose membranes (Bio-Rad, Hercules, CA) and blocking with 2% bovine serum albumin (Sigma) in PBS (pH 7.4), the membranes were incubated with the indicated primary antibodies overnight at 4 °C, followed by incubation with appropriate horseradish peroxidase (HRP) conjugated secondary antibody. The proteins were subsequently detected using ECL plus from Amersham (Piscataway, NJ) and/or SuperSignal West Femptomax sensitivity substrate from Pierce (Rockford, IL). Quantitative immunoblots were performed by accompanying lysate samples with a standard curve of pure proteins for densitometric analysis.

Macrophage Killing Assays. RAW 264.7 macrophages transfected with empty vector, DNA encoding CaM (i.e., RAW^{CaM}), or the divalent cation transporter Nramp1 (i.e., RAW^{Nramp1}) were challenged with *S. typhimurium* at a multiplicity of infection of 100, essentially as previously described (*30*, *38*). Briefly, *S. typhimurium* 14028 cells were cultured the day before the assay in LB broth at 37 °C overnight and were harvested by centrifugation (12000 rpm for 1 min) before resuspension at a final density of 5×10^5 cells/mL in 24-well cell culture plates. Prior to bacterial challenge, macrophages were primed with 100 units/mL interferon γ (IFNγ) and rinsed, and the prepared *S. typhimurium*-laden media were directly added to the plate of macrophages (*39*). The infection proceeded as plates were placed back into the incubator under standard conditions (37 °C in 5% CO_2). Following incubation for 30 min to permit macrophages to phagocytize the *S. typhimurium*, extracellular bacteria were rinsed off with PBS. Fresh media (12.5 μg of gentamicin/mL) replaced the bacteria-laden media to eliminate extracellular bacteria and prevent the extracellular replication and invasion of any *S. typhimurium* remaining on the plate. Macrophages infected with *S. typhimurium* were then further incubated, and at indicated times cells were washed and lysed [PBS, 1% Triton X-100, and 0.1% sodium dodecyl sulfate (SDS) for 5 min at room temperature]. Remaining viable bacteria were detected following the serial dilution of the cellular lysates onto LB agarose plates that were incubated overnight at 37 °C. Visible colonies were counted the following day, which reflected the level of viable bacteria still remaining in the macrophage after the designated time of infection.

RESULTS

Time-Dependent Changes in CaM Abundance upon Macrophage Activation. Following cellular lysis of RAW 264.7 macrophages, CaM is detected as a 16 kDa band on Western immunoblots of lysates from RAW 264.7 macrophages and is estimated to represent approximately 0.04% of total cellular protein (i.e., 25 pmol of CaM/mg of cell lysate) using an authentic CaM standard (Figure 1). There is a rapid increase in CaM abundance following exposure of macrophages to LPS bacterial endotoxin (10 ng/mL), which reaches an apparent maximum during the first 30 min and subsequently returns to a level characteristic of the quiescent cells. Analysis of the cytosolic and membrane fractions of the cell lysates indicates that the CaM increase is not caused by translocation of CaM from the membrane to the cytosol. In fact, the amount of CaM that remained bound to the membrane following LPS treatment represented <20% of the total CaM (data not shown), indicating that this population of bound CaM could not account for the large increase in CaM abundance apparent using Western immunoblots to probe cellular lysates.

Specific inhibitors were identified that block the LPS-dependent increase in CaM abundance to identify the underlying mechanisms. The LPS-dependent increase in CaM abundance was prevented by adding the translation inhibitor cyclohexamide (100 units/mL), which blocks the translocation step of the ribosome (Figure 1, yellow diamonds). Likewise, the LPS-dependent increase in CaM abundance was blocked by adding the inhibitor of transcription actinomycin D (5 μM) (Figure 1, white triangles). At this concentration, actinomycin D is a specific inhibitor that acts by complexing with deoxyguanosine residues on DNA to interfere with RNA polymerase by blocking its movement (*40*). These results indicate that LPS induces CaM expression on a rapid time scale (i.e., within 30 min). Because the time scale of LPS-mediated changes in CaM abundance are

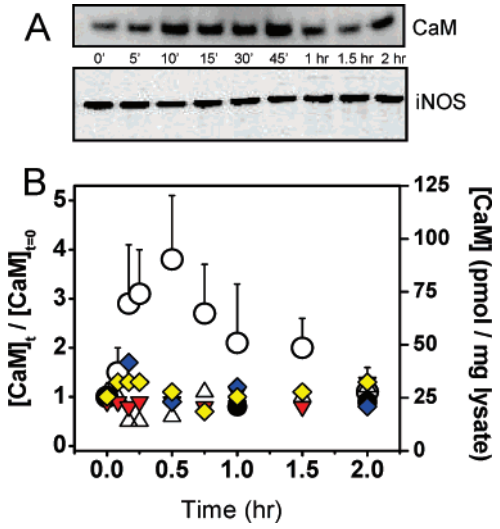

FIGURE 1: Immunoblots showing CaM and iNOS abundance changes following macrophage challenge with LPS (A) and densitometric analysis (B) for untreated control (●), following addition of the endotoxin lipopolysaccharide (LPS) (10 ng/mL) (○), following addition of LPS and an inhibitor of transcription (actinomycin D, 5 μM) (△), following addition of LPS and an inhibitor of protein synthesis (cyclohexamide, 100 μg/mL) (yellow ◆), following addition of LPS and an inhibitor of NFκB transcriptional activation (sulfasalazine, 2 mM) (red ▼), and following addition of LPS and a proteasome inhibitor (lactacystin, 1 μM) (blue ◆). For comparison, an immunblot against iNOS using antibody sc-650 is shown. Absolute abundance of CaM was measured from quantitative immunoblots using purified CaM as a standard and normalized against a GAPDH standard. Averages and standard deviations are for five independent biological replicates, in which at least two Western blots were used to analyze each time course (i.e., $n > 10$). All blots were normalized to GAPDH abundance, and blots were used only if the total variance of this loading standard was less than 20%. Observed increases in CaM abundance following LPS exposure are significant, as measured using a one population *t*-test, where $p < 0.0005$. For clarity, error bars are only shown for samples following exposure to LPS in the absence of inhibitors.

consistent with prior measurements of changes in the abundance of key cellular regulators of the inflammatory response, such as the transcription factor NFκB (*41*), these results suggest a coordination between changes in CaM expression and the inflammatory response.

To explore the possible role of NFκB in mediating CaM gene transcription, we have investigated the possibility that the NFκB inhibitor sulfasalazine might prevent the LPS-dependent increase in CaM abundance. Sulfasalazine is a synthetic compound that contains the antibiotic sulfapyridine and the antiinflammatory agent 5-aminosalicylic acid. Sulfasalazine is known to specifically inhibit NFκB by preventing its translocation into the nucleus (*42*). We found that pretreatment of RAW 264.7 cells with sulfasalazine (2 mM) prevented LPS-dependent increases in CaM abundance (Figure 1, red inverted triangles). These results suggest a direct linkage between the activation of NFκB and increases in CaM abundance and support a model in which LPS-dependent changes in CaM abundance are linked to the global inflammatory response. Wahl and co-workers demonstrated that the hallmark proteins induced with LPS stimulation were not present when NFκB was inhibited with sulfasalazine treatment (*42*).

To further explore the linkage between NFκB activation and changes in CaM abundance, we have selectively

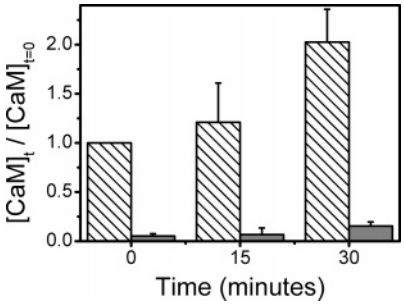

FIGURE 2: Diminished CaM abundance upon inhibition of NFκB. Comparison of CaM abundances in wild-type RAW 264.7 (hatched) and stably transfected cells containing dominant-negative IκBα (gray shading) before and following addition of endotoxin lipopolysaccharide (LPS) (10 ng/mL) measured from the density of CaM bands as described in the legend to Figure 1. Dominant-negative IκBα forms a stable inactive complex with NFκB. Error bars represent the standard deviation for three independent measurements.

inhibited the proteasome using lactacystin (1 μM), because the proteasome-dependent degradation of the NFκB inhibitor IκB is necessary for NFκB nuclear translocation (*43*−*45*). Following inhibition of the proteasome, the LPS-dependent increase in CaM protein abundance was abolished (Figure 1, blue diamonds), further suggesting an important role for NFκB. Additional evidence indicating a causal linkage between the nuclear localization of NFκB and changes in CaM abundance is apparent from a consideration of the effects of a dominant-negative form of IκB (i.e., IκBαM). In this IκB mutant, sites associated with IκB kinase phosphorylation are mutated to prevent NFκB activation and nuclear localization. In comparison to wild-type RAW cells, there is a 95% decrease in CaM abundance following expression of the dominant-negative mutant of IκB (Figure 2). Following exposure to LPS the abundance of CaM remains very low. Taken together, these data indicate that the increase in CaM abundance, caused by LPS exposure, is through an NFκB-mediated increase in gene expression. Indeed, prior measurements have established an important role for NFκB in mediating the expression of iNOS, and there is an absolute requirement for CaM binding to both activate iNOS and to stabilize it against proteolytic digestion that may involve a calpain I cleavage site within the CaM-binding sequence (*46*). However, using commercially available antibodies against iNOS, we observe no LPS-dependent increase in iNOS abundance during the first 2 h (Figure 1). These results suggest that CaM expression may precede that of iNOS.

SDS−*PAGE Detection of CaM-Bound iNOS*. To better understand the coordinated regulation of iNOS and its activator CaM and their relationship to macrophage activation, we have investigated the possibility that there are differences in the relative abundances of the activated complex between CaM and iNOS relative to the inactive form of iNOS, in which CaM is not bound, following the LPS-dependent activation of macrophages. Prior measurements indicate that the high-affinity complex between CaM and iNOS remains tightly associated following SDS−PAGE, irrespective of boiling or detergent solubilization (*47*), permitting us to assess the ability of commercially available antibodies to resolve the CaM-free and CaM-bound forms of iNOS. Indeed, using purified iNOS, we resolved two bands on SDS−PAGE with apparent molecular masses of ~130

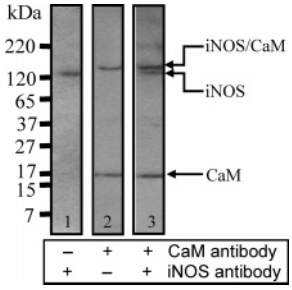

FIGURE 3: Immunoblots of purified recombinant iNOS (35 ng) and CaM (75 ng) separated by SDS−PAGE and probed using antibodies against iNOS (lane 1) and CaM (lane 2) and against both proteins simultaneously (lane 3). Apparent masses are approximately 16, 130, and 150 kDa for CaM, iNOS, and iNOS/CaM, in close agreement with the theoretical masses of 16706 (P62204) and 130575 (P29477) for these mouse proteins. Immunoblots were obtained using antibodies sc-5537 against CaM and sc-650 against iNOS. Similar results were obtained using five other commerically available antibodies, which were all made against peptides from the iNOS sequence (see Experimental Procedures).

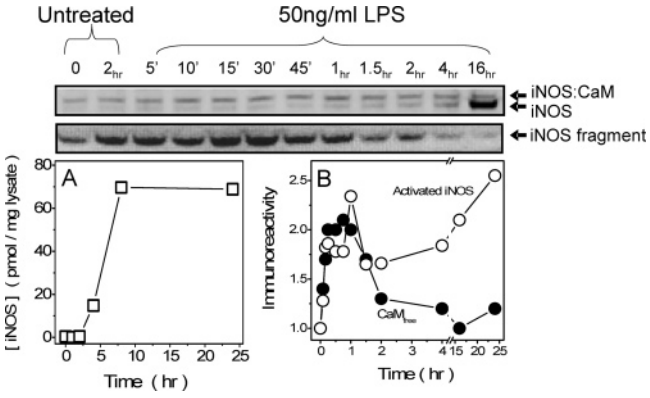

FIGURE 4: LPS-dependent changes in the relative abundance of uncomplexed (A) and CaM-bound (activated) iNOS (B) following separation of 15 μg of cellular lysate by SDS−PAGE and immunoblot detection (top) and associated densitometric analysis for unbound iNOS (□) using authentic iNOS standards (A) and changes in immunoreactivity of the complex between iNOS and CaM (B) (○) relative to changes in the abundance of unbound (free) CaM (●) (B). Immunoblots show the complex between CaM and iNOS (i.e., 150 kDa iNOS/CaM complex detected using antibody sc-5537) and unbound full-length 130 kDa iNOS or 60 kDa iNOS fragment (i.e., iNOS or iNOS fragment detected using antibody sc-650).

and 150 kDa that are consistent with the masses of the uncomplexed and CaM-bound forms of iNOS. The 130 kDa band was detected using any one of six commercial antibodies tested against iNOS (see Experimental Procedures) (Figure 3). The 150 and 17 kDa bands are both immunoreactive using the antibody against CaM. The high molecular mass iNOS complex can thus be detected using antibodies against CaM, but not with any of the commercially available antibodies against iNOS. The inability of antibodies raised against peptides from iNOS to detect the active complex between CaM and iNOS probably reflects the stabilization of the iNOS structure, which modulates the exposure of epitopes near the amino and carboxyl termini of iNOS to affect antibody recognition, consistent with prior measurements that indicate CaM binding induces allosteric structural changes between the reductase and oxidase domains of iNOS (*48*−*53*). These results suggest that prior measurements showing a requirement of 4 h for significant upregulation of iNOS abundance following exposure of macrophages to LPS may have selectively detected the CaM-free (inactive) form of iNOS.

Coordinated Abundance Changes in CaM and Complex with iNOS. Because known prior measurements have relied on antibodies against iNOS to measure LPS-dependent increases in iNOS protein abundance, and our commercially available antibodies do not recognize activated iNOS bound to CaM (see above), we have reinvestigated the time-dependent changes in iNOS abundance following LPS stimulation of macrophages using our new assay that involves the combined use of antibodies raised against both CaM and iNOS. Prior to LPS exposure, a single major band is apparent corresponding to the complex between CaM and iNOS (Figure 4, top). This 150 kDa species is the only CaM-associated complex seen in macrophage lysate following separation and visualization on SDS−PAGE. In response to LPS exposure, there was a rapid 2-fold increase in the abundance of the active iNOS/CaM complex, which occurs on a similar time scale to observed LPS-dependent increases in CaM abundance (Figure 4B). Consistent with prior reports, there are no significant changes in the abundance of the uncomplexed (i.e., CaM-free) form of iNOS during the first several hours following LPS exposure (*4*, *31*−*34*). The abundance of uncomplexed iNOS increases following 4 h of LPS exposure (Figure 4A). The total amount of uncomplexed iNOS apparent at long times (i.e., $t > 4$ h) following LPS exposure was calculated using authentic standards to be ∼70 pmol/mg of cell lysate, which exceeds the available amount of unbound CaM (see Figure 1). The similar amplitude and kinetics associated with LPS-dependent increases in the abundances of CaM and CaM-bound iNOS are consistent with a mechanism whereby CaM binding stabilizes iNOS from rapid degradation (*46*). Consistent with this interpretation, there is a time-dependent decrease in the abundance of a 60 kDa iNOS fragment that correlates with increases in CaM abundance and the stabilization of the CaM/iNOS complex (Figure 4). Likewise, inhibition of the proteasome after LPS activation and the generation of message leads to the accumulation of iNOS (*54*), indicating that the proteasome-dependent pathway of degradation functions to mediate the degradation of iNOS.

CaM Overexpression Stabilizes iNOS. Identification of the linkage between CaM expression and the formation of the CaM/iNOS complex was clarified following the stable transfection of RAW 264.7 cells with CaM cDNA (RAW-^{CaM}), which is fully described in Experimental Procedures. In the RAW^{CaM} cells, there was an approximate 2-fold increase in CaM abundance assayed as the immunoreactivity of the 16 kDa band following protein separation by SDS−PAGE (Figure 5A). There is a corresponding increase in the immunoreactivity of the major 150 kDa upper band corresponding to the complex between CaM and iNOS. These results indicate that increases in CaM abundance stabilize iNOS and result in an increase in its cellular abundance. The complex between CaM and iNOS is fully active, and there is direct correlation between the increase in the abundance of the CaM/iNOS complex and catalytic function (i.e., nitric oxide generated) (Figure 5B). Furthermore, overexpression of CaM and the stabilization of the complex between CaM and iNOS act to reduce the rate of iNOS degradation (Figure 5C,D). This latter interpretation is consistent with the

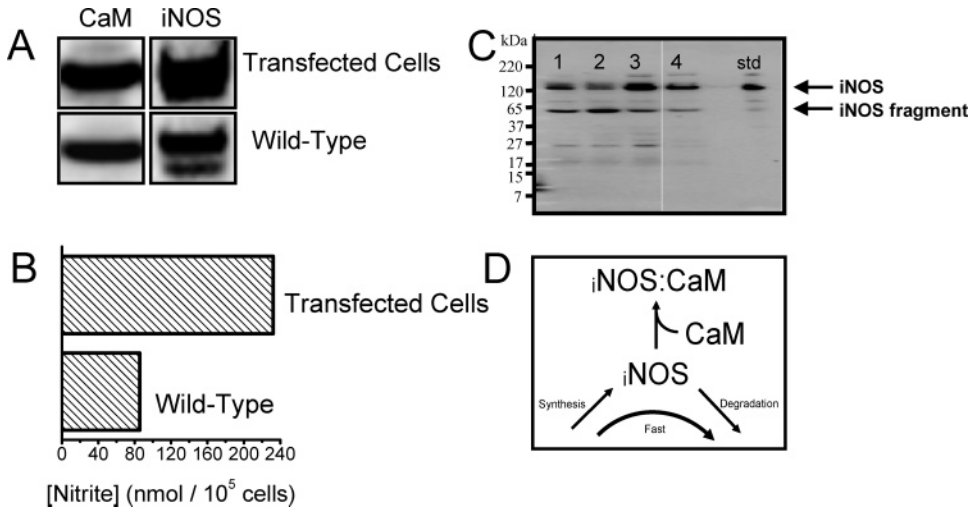

FIGURE 5: Immunoblots demonstrating (A) linkage between CaM overexpression and iNOS abundance for wild-type and transfected RAW264.7 cells containing the pcDNA3.1 vector encoding CaM and (B) nitric oxide generation from iNOS measured as total nitrite using the Griess reagent. (C) Comparison between total iNOS expression levels for 15 μg of cell lysate from wild-type cells (lane 1) or cells transfected with empty vector alone (lane 2), vector encoding CaM (lane 3), and vector encoding the divalent cation transporter Nramp1 (lane 4) following macrophage overnight stimulation with IFNγ (100 units/mL). Authentic iNOS standard (185 ng) is shown in the far right lane. (D) Scheme illustrating the role of CaM abundance in stabilizing the activated iNOS/CaM complex.

presence of a calpain cleavage site present in the CaM-binding sequence of iNOS (*46*).

CaM-Dependent Bacterial Killing. To further clarify the role of the activated form of iNOS on macrophage function, we have investigated how CaM overexpression and the stabilization of iNOS affect the time course of bacterial infection by *S. typhimurium*. For comparison purposes, we have also considered how the overexpression of natural resistance-associated macrophage protein 1 (Nramp1), which is a divalent cation transporter that has previously been implicated in mediating host resistance (*55*), affects bacterial killing. Prior to infection, macrophages were primed with the cytokine interferon-γ (IFN-γ), which is known to upregulate iNOS gene expression (*56*). The abundance of iNOS was measured by Western immunoblots, which revealed the expected correlation between CaM overexpression and an increased abundance of iNOS relative to either control or cells transfected using an empty vector that does not encode CaM (Figure 5C). In all cases a fragment of iNOS is apparent that is also visible in the authentic purified iNOS standard. However, in comparison to the control cells or those transfected with the empty vector, there is a substantial reduction in the immunostaining of the iNOS fragment upon overexpression of CaM. Similar increases in the abundance of iNOS and reductions in the iNOS fragment are apparent in cells transfected with Nramp1 (i.e., RAW^{Nramp1}), which is known to have an increased resistance to bacterial infection (*57*). Nramp1 is known to increase both the abundance of the transcription factor IRF1 and IRF1 promoter binding affinity (*55*), and given that there are IRF1 binding sites in both iNOS and CaM promoters, Nramp1 expression is expected to upregulate the expression of both iNOS and CaM to enhance the formation of the functional stable complex associated with the observed bactericidal activity (*58*, *59*). These results support the suggestion that increases in iNOS abundance upon CaM overexpression are the result of iNOS stabilization and an associated reduction in the rate of its degradation.

To assess the functional significance of observed CaM-dependent increases in iNOS abundance and the physiological role of the complex between CaM and iNOS in mediating bacterial killing, macrophages were exposed to *S. typhimurium*. Control RAW 264.7 cells (or empty vector controls) were rapidly colonized by *S. typhimurium*, and there is a time-dependent increase in the number of viable bacterial colonies following infection (Figure 6). In contrast, macrophages overexpressing CaM (i.e., RAW^{CaM}) rapidly cleared the internalized bacteria; after 2 h there were <20% of the bacterial colonies present immediately after infection. Macrophages overexpressing Nramp1 (i.e., RAW^{Nramp1}) exhibited a similar bactericidal activity to that associated with the CaM-overexpressing clones, suggesting that the observed increase in stabilized iNOS represents a possible common mechanism for the efficient elimination of intracellular bacteria from macrophages.

DISCUSSION

We have demonstrated a rapid upregulation of CaM-bound iNOS protein levels within the first 30 min following the activation of RAW 264.7 macrophages with LPS (Figure 4B) that occurs on a much faster time scale than that associated with the detection of uncomplexed iNOS (Figure 4A). Indeed, all prior measurements suggest that increases in iNOS protein abundance requires 4 h after LPS exposure (*4*, *31*−*34*). Mechanistically, increases in CaM protein abundance function to stabilize iNOS protein, and equivalent increases in CaM-bound iNOS appear in response to a 2-fold increase in CaM abundance following either LPS exposure or the overexpression of CaM (Figures 4B and 5A). Further, observed increases in the abundance of the complex between CaM and iNOS are functionally important, as is apparent from the increased generation of $NO^{\bullet}$ (Figure 5B) and enhanced bactericidal activity of macrophages overexpressing CaM (Figure 6). Inhibition of the proteasome using lactacystin blocks observed increases in CaM expression in response to LPS treatment, as does low concentrations of

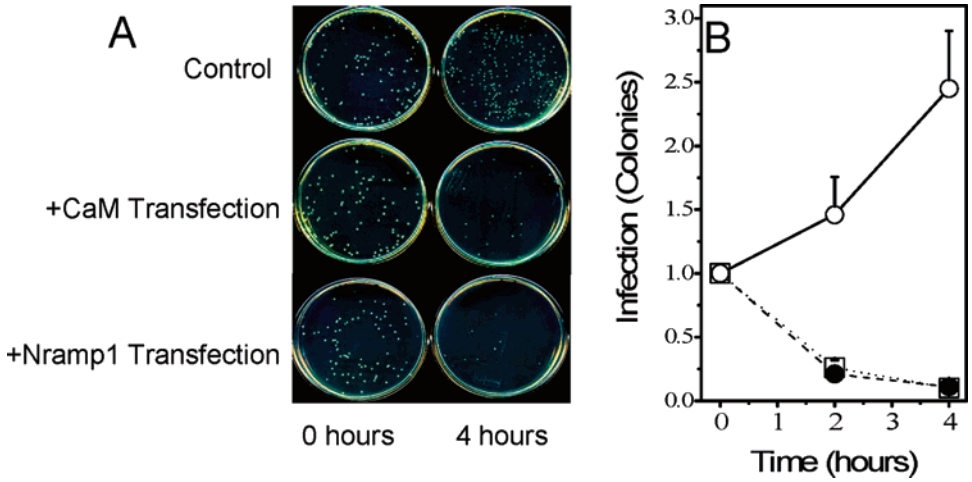

FIGURE 6: *Salmonella typhimurium* colony formation (A) and associated quantitation (B) following infection of wild-type (control) cells (○) or transfected cells overexpressing either CaM (●) or Nramp1 (□) (5×10^5 cells/mL) with approximately 5×10^7 *S. typhimurium* cells. Extracellular bacteria were eliminated after 30 min (see Experimental Procedures), and at indicated times macrophages were lysed and bacteria were counted manually following overnight incubation of serially diluted lysate on LB plates to allow the formation of visible bacterial colonies. Error bars represent the standard error of the mean for three replicates.

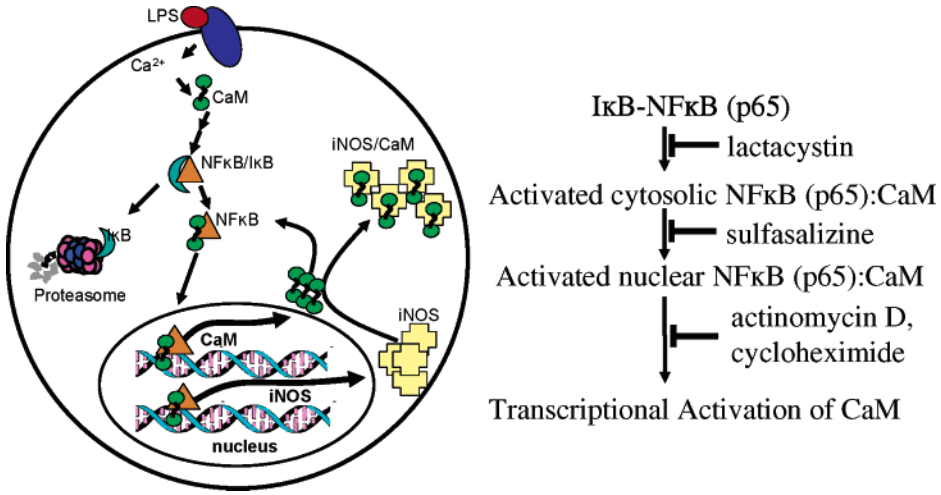

FIGURE 7: Model summarizing LPS-dependent increases in the abundances of CaM and iNOS associated with respiratory burst in macrophages. Following LPS binding to toll-like receptors, increases in cytosolic calcium promotes CaM activation, which is known to bind NFκB family members and modulate their nuclear localization (*4*, *62*, *72*, *73*). Inhibitors of NFκB (i.e., sulfasalazine) block LPS-dependent increases in CaM, as does specific inhibition of the proteasome (i.e., lactacystin) or inhibition of the degradation of IκB (see Figure 1). Following nuclear localization of NFκB there is an upregulation of CaM gene expression and protein translation, which are respectively blocked by actinomycin D and cycloheximide (see Figure 1). CaM binding to expressed iNOS results in its activation and prevents calpain-dependent degradation that normally functions to maintain low levels of iNOS.

the inhibitor sulfasalizine, which both act to block NFκB nuclear localization and transcriptional activaiton (Figure 1). Likewise, expression of a dominant-negative construct of IκB results in dramatic reductions in CaM abundance (Figure 2). These latter results are consistent with a central role for NFκB in mediating CaM expression, because the nuclear localization of NFκB requires the proteasome-dependent degradation of the inhibitory subunit IκB (*60*, *61*) (Figure 7). Furthermore, nuclear localization of the NFκB family member c-Rel is retarded upon CaM binding (*62*), providing possible feedback regulatory control to downregulate NFκB-mediated gene regulation through increases in CaM expression levels. In conclusion, our results provide strong evidence that increases in CaM expression levels occur early during macrophage activation and indicate an unappreciated regulation of macrophage function by CaM. This regulation rapidly upregulates the generation of nitric oxide by forming a stable complex with iNOS, a protein which plays a critical role in conjunction with other key enzymes (i.e., NADPH oxidase) in mediating the oxidative burst and bacterial killing (*63*).

A functional requirement for CaM binding to a conserved sequence connecting the N-terminal oxygenase and C-terminal reductase domains of iNOS has been recognized for some time, as CaM is a critical cofactor whose binding to iNOS promotes enzyme activation (*23*, *48*, *64*, *65*). Further, in the absence of bound CaM, whose binding to iNOS blocks its proteolytic digestion, expressed iNOS is rapidly degraded by endogenous proteases (*4*, *31*−*34*). However, prior measurements have failed to appreciate that commercially available antibodies fail to detect the CaM-bound (activated) form of iNOS present in macrophages, but rather selectively monitor the uncomplexed and inactive form of iNOS (Figure 3). For this reason, the rapid upregulation of the CaM/iNOS complex has not been detected. The inability to detect functional CaM-bound iNOS has confounded an understanding of the role of iNOS in mediating

the bactericidal activity of macrophages, as reactive nitrogen species are detected within the first hour following LPS stimulation (*30*). Our results indicate that CaM upregulation and binding to iNOS, which forms a stabilized and active complex that is not recognized for degradation, result in an increased abundance of the CaM/iNOS complex. Further, the coordinate upregulation of CaM and its complex with iNOS within the first 30 min following LPS exposure, coupled with the fact that stabilization of the CaM/iNOS complex promotes effective bacterial killing (Figure 6), indicates that the CaM/iNOS complex plays an important early role in the host immune response. Because the stabilization of the CaM/iNOS complex occurs on the same time scale as the oxidative burst (*63*, *66*, *67*), it is expected that CaM/iNOS and NADPH oxidase function in a coordinated manner, whereby the combined generation of $NO^{\bullet}$ and $O_2^{\bullet-}$ mediate bacterial killing. Indeed, $NO^{\bullet}$ and $O_2^{\bullet-}$ are long-lived and mildly reactive species that have the potential to combine in a diffusion-limited reaction to form peroxynitrite and other highly reactive species having the ability to rapidly oxidize and inactivate host proteins (*68*, *69*). At longer times, the cellular abundance of iNOS exceeds that of CaM (Figures 1 and 4A) and exists primarily as a monomer that can approach 1.6% of the total cellular protein (*70*). Under these latter conditions, essentially all available CaM is bound to expressed iNOS, and limiting CaM levels induces activated macrophages to undergo cellular apoptosis to effectively limit collateral tissue damage (*4*).

The importance of increased CaM expression is apparent from functional measurements, which indicate that CaM-overexpressing macrophages effectively recognize and kill internalized *S. typhimurium* (Figure 6). In contrast, wild-type RAW 264.7 macrophages are much more rapidly colonized by *Salmonella*, emphasizing the functional importance of bacterial-induced changes in CaM expression levels to the ability of macrophages to mediate the oxidative burst associated with bacterial killing. As indicated, the fundamental reason associated with the ability of CaM-expressing macrophages to inhibit bacterial growth is related to the stabilization of functional iNOS, whose degradation is prevented following CaM expression (Figure 5D). Indeed, similar levels of bacterial killing are observed using macrophages that have been transfected with Nramp1, resulting in a similar increase in iNOS protein abundance (Figure 6). Further coordinated changes in gene expression associated with CaM upregulation also occur, whereby upon overexpression of CaM, dramatic reductions occur in the nuclear localization and activation of key transcription factors (i.e., p65, phosphorylated c-Jun, and Sp1). Such reductions have associated decreases in the abundance of key inflammatory cytokines (i.e., TNFα) following LPS exposure that minimize apoptotic responses (*4*). These latter results suggest that signaling pathways are shifted away from the apoptotic response as a result of CaM association with critical binding partners. Indeed, use of TNFα-specific siRNA results in a dramatic decrease in apoptosis because of a downregulation of iNOS gene expression (*4*). Furthermore, upon downregulation of TNFα expression levels, one observes a corresponding decrease in iNOS. Thus, important feedback mechanisms coordinate the generation of the oxidative burst associated with iNOS induction and bacterial killing. Indeed, observed age-dependent decreases in nitric oxide production by activated macrophages may be attributed to losses of functional CaM/iNOS complexes, as the abundance and function of CaM are diminished during biological aging (*15*, *17*, *19*, *20*, *71*).

ACKNOWLEDGMENT

We thank Diana J. Bigelow, Banu Gopalan, M. Uljana Mayer, Brian D. Thrall, Sewite Negash, and Thomas J. Weber for insightful discussions.

REFERENCES

1. De La Fuente, M. (1985) Changes in the macrophage function with aging, *Comp. Biochem. Physiol. A 81*, 935−938.
2. Lloberas, J., and Celada, A. (2002) Effect of aging on macrophage function, *Exp. Gerontol. 37*, 1325−1331.
3. Plowden, J., Renshaw-Hoelscher, M., Engleman, C., Katz, J., and Sambhara, S. (2004) Innate immunity in aging: impact on macrophage function, *Aging Cell 3*, 161−167.
4. Weber, T. J., Smallwood, H. S., Kathmann, L. E., Markillie, L. M., Squier, T. C., and Thrall, B. D. (2006) Functional linkage between tumor necrosis factor biosynthesis and calmodulin-dependent activation of iNOS in RAW 264.7 macrophages, *Am. J. Physiol. Cell Physiol. 290*, C1512−C1520.
5. Cannon, J. G. (1998) Intrinsic and extrinsic factors in muscle aging, *Ann. N.Y. Acad. Sci. 854*, 72−77.
6. Kitagawa, S., Yuo, A., Yagisawa, M., Azuma, E., Yoshida, M., Furukawa, Y., Takahashi, M., Masuyama, J., and Takaku, F. (1996) Activation of human monocyte functions by tumor necrosis factor: rapid priming for enhanced release of superoxide and erythrophagocytosis, but no direct triggering of superoxide release, *Exp. Hematol. 24*, 559−567.
7. Resto-Ruiz, S. I., Schmiederer, M., Sweger, D., Newton, C., Klein, T. W., Friedman, H., and Anderson, B. E. (2002) Induction of a potential paracrine angiogenic loop between human THP-1 macrophages and human microvascular endothelial cells during Bartonella henselae infection, *Infect. Immun. 70*, 4564−4570.
8. Forman, H. J., and Torres, M. (2002) Reactive oxygen species and cell signaling: respiratory burst in macrophage signaling, *Am. J. Respir. Crit. Care Med. 166*, S4−S8.
9. Karupiah, G., Hunt, N. H., King, N. J., and Chaudhri, G. (2000) NADPH oxidase, Nramp1 and nitric oxide synthase 2 in the host antimicrobial response, *Rev. Immunogenet. 2*, 387−415.
10. Barbieri, S. S., Eligini, S., Brambilla, M., Tremoli, E., and Colli, S. (2003) Reactive oxygen species mediate cyclooxygenase-2 induction during monocyte to macrophage differentiation: critical role of NADPH oxidase, *Cardiovasc. Res. 60*, 187−197.
11. Cassatella, M. A., Della Bianca, V., Berton, G., and Rossi, F. (1985) Activation by gamma interferon of human macrophage capability to produce toxic oxygen molecules is accompanied by decreased K_m of the superoxide-generating NADPH oxidase, *Biochem. Biophys. Res. Commun. 132*, 908−914.
12. Johnson, W. J., and Sung, C. P. (1987) Rat macrophage treatment with lipopolysaccharide leads to a reduction in respiratory burst product secretion and a decrease in NADPH oxidase affinity, *Cell Immunol. 108*, 109−119.
13. Mutunga, M., Graham, S., De Hormaeche, R. D., Musson, J. A., Robinson, J. H., Mastroeni, P., Khan, C. M., and Hormaeche, C. E. (2004) Attenuated *Salmonella typhimurium* htrA mutants cause fatal infections in mice deficient in NADPH oxidase and destroy NADPH oxidase-deficient macrophage monolayers, *Vaccine 22*, 4124−4131.
14. Malik, Z. A., Iyer, S. S., and Kusner, D. J. (2001) *Mycobacterium tuberculosis* phagosomes exhibit altered calmodulin-dependent signal transduction: contribution to inhibition of phagosome-lysosome fusion and intracellular survival in human macrophages, *J. Immunol. 166*, 3392−3401.
15. Gao, J., Yin, D., Yao, Y., Williams, T. D., and Squier, T. C. (1998) Progressive decline in the ability of calmodulin isolated from aged brain to activate the plasma membrane Ca-ATPase, *Biochemistry 37*, 9536−9548.
16. Logan, S., Cameron, J. A., and Vig, P. J. (2003) Calmodulin activity in aging rat heart, *Biomed. Sci. Instrum. 39*, 561−566.
17. Teolato, S., Calderini, G., Bonetti, A. C., and Toffano, G. (1983) Calmodulin content in different brain areas of aging rats, *Neurosci. Lett. 38*, 57−60.

18. Bigelow, D. J., and Squier, T. C. (2005) Redox modulation of cellular signaling and metabolism through reversible oxidation of methionine sensors in calcium regulatory proteins, *Biochim. Biophys. Acta 1703*, 121−134.
19. Lu, T., Pan, Y., Kao, S. Y., Li, C., Kohane, I., Chan, J., and Yankner, B. A. (2004) Gene regulation and DNA damage in the ageing human brain, *Nature 429*, 883−891.
20. Toda, T., Morimasa, T., Kobayashi, S., Nomura, K., Hatozaki, T., and Hirota, M. (2003) A proteomic approach to determination of the significance of protein oxidation in the ageing of mouse hippocampus, *Appl. Genomics Proteomics 2*, 43−50.
21. Broeke, R. T., Leusink-Muis, T., Hilberdink, R., Van Ark, I., van den Worm, E., Villain, M., De Clerck, F., Blalock, J. E., Nijkamp, F. P., and Folkerts, G. (2004) Specific modulation of calmodulin activity induces a dramatic production of superoxide by alveolar macrophages, *Lab. Invest. 84*, 29−40.
22. Rikihisa, Y., Zhang, Y., and Park, J. (1995) Role of Ca^{2+} and calmodulin in ehrlichial infection in macrophages, *Infect. Immun. 63*, 2310−2316.
23. Gribovskaja, I., Brownlow, K. C., Dennis, S. J., Rosko, A. J., Marletta, M. A., and Stevens-Truss, R. (2005) Calcium-binding sites of calmodulin and electron transfer by inducible nitric oxide synthase, *Biochemistry 44*, 7593−7601.
24. Yap, K. L., Kim, J., Truong, K., Sherman, M., Yuan, T., and Ikura, M. (2000) Calmodulin target database, *J. Struct. Funct. Genomics 1*, 8−14.
25. Shen, X., Valencia, C. A., Szostak, J. W., Dong, B., and Liu, R. (2005) Scanning the human proteome for calmodulin-binding proteins, *Proc. Natl. Acad. Sci. U.S.A. 102*, 5969−5974.
26. Persechini, A., and Stemmer, P. M. (2002) Calmodulin is a limiting factor in the cell, *Trends Cardiovasc. Med. 12*, 32−37.
27. Tran, Q. K., Black, D. J., and Persechini, A. (2003) Intracellular coupling via limiting calmodulin, *J. Biol. Chem. 278*, 24247−24250.
28. Tran, Q. K., Black, D. J., and Persechini, A. (2005) Dominant affectors in the calmodulin network shape the time courses of target responses in the cell, *Cell Calcium 37*, 541−553.
29. Vazquez-Torres, A., and Fang, F. C. (2001) Oxygen-dependent anti-*Salmonella* activity of macrophages, *Trends Microbiol. 9*, 29−33.
30. Vazquez-Torres, A., Jones-Carson, J., Mastroeni, P., Ischiropoulos, H., and Fang, F. C. (2000) Antimicrobial actions of the NADPH phagocyte oxidase and inducible nitric oxide synthase in experimental salmonellosis. I. Effects on microbial killing by activated peritoneal macrophages in vitro, *J. Exp. Med. 192*, 227−236.
31. Srisook, K., and Cha, Y. N. (2004) Biphasic induction of heme oxygenase-1 expression in macrophages stimulated with lipopolysaccharide, *Biochem. Pharmacol. 68*, 1709−1720.
32. Eriksson, S., Chambers, B. J., and Rhen, M. (2003) Nitric oxide produced by murine dendritic cells is cytotoxic for intracellular *Salmonella enterica* sv. *Typhimurium*, *Scand. J. Immunol. 58*, 493−502.
33. Linehan, S. A., and Holden, D. W. (2003) The interplay between *Salmonella typhimurium* and its macrophage host−what can it teach us about innate immunity?, *Immunol. Lett. 85*, 183−192.
34. Vallance, B. A., Deng, W., De Grado, M., Chan, C., Jacobson, K., and Finlay, B. B. (2002) Modulation of inducible nitric oxide synthase expression by the attaching and effacing bacterial pathogen citrobacter rodentium in infected mice, *Infect. Immun. 70*, 6424−6435.
35. Govoni, G., Canonne-Hergaux, F., Pfeifer, C. G., Marcus, S. L., Mills, S. D., Hackam, D. J., Grinstein, S., Malo, D., Finlay, B. B., and Gros, P. (1999) Functional expression of Nramp1 in vitro in the murine macrophage line RAW264.7, *Infect. Immun. 67*, 2225−2232.
36. Strasburg, G. M., Hogan, M., Birmachu, W., Thomas, D. D., and Louis, C. F. (1988) Site-specific derivatives of wheat germ calmodulin. Interactions with troponin and sarcoplasmic reticulum. *J. Biol. Chem. 263*, 542−548.
37. Qin, Z., and Squier, T. C. (2001) Calcium-dependent stabilization of the central sequence between Met(76) and Ser(81) in vertebrate calmodulin, *Biophys. J. 81*, 2908−2918.
38. Rosenberger, C. M., and Finlay, B. B. (2002) Macrophages inhibit *Salmonella typhimurium* replication through MEK/ERK kinase and phagocyte NADPH oxidase activities, *J. Biol. Chem. 277*, 18753−18762.
39. Garvis, S. G., Beuzon, C. R., and Holden, D. W. (2001) A role for the PhoP/Q regulon in inhibition of fusion between lysosomes and *Salmonella*-containing vacuoles in macrophages, *Cell Microbiol. 3*, 731−744.
40. Kamitori, S., and Takusagawa, F. (1992) Crystal structure of the 2:1 complex between d(GAAGCTTC) and the anticancer drug actinomycin D, *J. Mol. Biol. 225*, 445−456.
41. Chen, B. C., Chou, C. F., and Lin, W. W. (1998) Pyrimidinoceptor-mediated potentiation of inducible nitric-oxide synthase induction in J774 macrophages. Role of intracellular calcium, *J. Biol. Chem. 273*, 29754−29763.
42. Wahl, C., Liptay, S., Adler, G., and Schmid, R. M. (1998) Sulfasalazine: a potent and specific inhibitor of nuclear factor kappa B, *J. Clin. Invest. 101*, 1163−1174.
43. Scherer, D. C., Brockman, J. A., Chen, Z., Maniatis, T., and Ballard, D. W. (1995) Signal-induced degradation of I kappa B alpha requires site-specific ubiquitination, *Proc. Natl. Acad. Sci. U.S.A. 92*, 11259−11263.
44. Li, C. C., Dai, R. M., and Longo, D. L. (1995) Inactivation of NF-kappa B inhibitor I kappa B alpha: ubiquitin-dependent proteolysis and its degradation product, *Biochem. Biophys. Res. Commun. 215*, 292−301.
45. Chen, Z., Hagler, J., Palombella, V. J., Melandri, F., Scherer, D., Ballard, D., and Maniatis, T. (1995) Signal-induced site-specific phosphorylation targets I kappa B alpha to the ubiquitin-proteasome pathway, *Genes Dev. 9*, 1586−1597.
46. Walker, G., Pfeilschifter, J., Otten, U., and Kunz, D. (2001) Proteolytic cleavage of inducible nitric oxide synthase (iNOS) by calpain I, *Biochim. Biophys. Acta 1568*, 216−224.
47. Cho, H. J., Xie, Q. W., Calaycay, J., Mumford, R. A., Swiderek, K. M., Lee, T. D., and Nathan, C. (1992) Calmodulin is a subunit of nitric oxide synthase from macrophages, *J. Exp. Med. 176*, 599−604.
48. Alderton, W. K., Cooper, C. E., and Knowles, R. G. (2001) Nitric oxide synthases: structure, function and inhibition, *Biochem. J. 357*, 593−615.
49. Ghosh, D. K., Wu, C., Pitters, E., Moloney, M., Werner, E. R., Mayer, B., and Stuehr, D. J. (1997) Characterization of the inducible nitric oxide synthase oxygenase domain identifies a 49 amino acid segment required for subunit dimerization and tetrahydrobiopterin interaction, *Biochemistry 36*, 10609−10619.
50. Jones, R. J., Gao, Y. T., Simone, T. M., Salerno, J. C., and Smith, S. M. (2006) NADPH analog binding to constitutive nitric oxide activates electron transfer and NO synthesis, *Nitric Oxide 14*, 228−237.
51. Knudsen, G. M., Nishida, C. R., Mooney, S. D., and Ortiz de Montellano, P. R. (2003) Nitric-oxide synthase (NOS) reductase domain models suggest a new control element in endothelial NOS that attenuates calmodulin-dependent activity, *J. Biol. Chem. 278*, 31814−31824.
52. Newman, E., Spratt, D. E., Mosher, J., Cheyne, B., Montgomery, H. J., Wilson, D. L., Weinberg, J. B., Smith, S. M., Salerno, J. C., Ghosh, D. K., and Guillemette, J. G. (2004) Differential activation of nitric-oxide synthase isozymes by calmodulin-troponin C chimeras, *J. Biol. Chem. 279*, 33547−33557.
53. Spratt, D. E., Newman, E., Mosher, J., Ghosh, D. K., Salerno, J. C., and Guillemette, J. G. (2006) Binding and activation of nitric oxide synthase isozymes by calmodulin EF hand pairs, *FEBS J. 273*, 1759−1771.
54. Musial, A., and Eissa, N. T. (2001) Inducible nitric-oxide synthase is regulated by the proteasome degradation pathway, *J. Biol. Chem. 276*, 24268−24273.
55. Fritsche, G., Dlaska, M., Barton, H., Theurl, I., Garimorth, K., and Weiss, G. (2003) Nramp1 functionality increases inducible nitric oxide synthase transcription via stimulation of IFN regulatory factor 1 expression, *J. Immunol. 171*, 1994−1998.
56. Govoni, G., Gauthier, S., Billia, F., Iscove, N. N., and Gros, P. (1997) Cell-specific and inducible Nramp1 gene expression in mouse macrophages in vitro and in vivo, *J. Leukocyte Biol. 62*, 277−286.
57. Vidal, S., Gros, P., and Skamene, E. (1995) Natural resistance to infection with intracellular parasites: molecular genetics identifies Nramp1 as the Bcg/Ity/Lsh locus, *J. Leukocyte Biol. 58*, 382−390.
58. Kamijo, R., Harada, H., Matsuyama, T., Bosland, M., Gerecitano, J., Shapiro, D., Le, J., Koh, S. I., Kimura, T., Green, S. J., Mak, T. W., Taniguchi, T., and Vilcek, J. (1994) Requirement for transcription factor IRF-1 in NO synthase induction in macrophages, *Science 263*, 1612−1615.

59. Martin, E., Nathan, C., and Xie, Q. W. (1994) Role of interferon regulatory factor 1 in induction of nitric oxide synthase, *J. Exp. Med. 180*, 977−984.
60. Hellerbrand, C., Jobin, C., Iimuro, Y., Licato, L., Sartor, R. B., and Brenner, D. A. (1998) Inhibition of NFkappaB in activated rat hepatic stellate cells by proteasome inhibitors and an IkappaB super-repressor, *Hepatology 27*, 1285−1295.
61. Kretz-Remy, C., Bates, E. E., and Arrigo, A. P. (1998) Amino acid analogs activate NF-kappaB through redox-dependent IkappaB-alpha degradation by the proteasome without apparent IkappaB-alpha phosphorylation. Consequence on HIV-1 long terminal repeat activation, *J. Biol. Chem. 273*, 3180−3191.
62. Antonsson, A., Hughes, K., Edin, S., and Grundstrom, T. (2003) Regulation of c-Rel nuclear localization by binding of Ca^{2+}/calmodulin, *Mol. Cell. Biol. 23*, 1418−1427.
63. Bureau, C., Bernad, J., Chaouche, N., Orfila, C., Beraud, M., Gonindard, C., Alric, L., Vinel, J. P., and Pipy, B. (2001) Nonstructural 3 protein of hepatitis C virus triggers an oxidative burst in human monocytes via activation of NADPH oxidase, *J. Biol. Chem. 276*, 23077−23083.
64. Bredt, D. S., and Snyder, S. H. (1990) Isolation of nitric oxide synthetase, a calmodulin-requiring enzyme, *Proc. Natl. Acad. Sci. U.S.A. 87*, 682−685.
65. MacMicking, J., Xie, Q. W., and Nathan, C. (1997) Nitric oxide and macrophage function, *Annu. Rev. Immunol. 15*, 323−350.
66. Ryan, K. A., Smith, M. F., Jr., Sanders, M. K., and Ernst, P. B. (2004) Reactive oxygen and nitrogen species differentially regulate Toll-like receptor 4-mediated activation of NF-kappa B and interleukin-8 expression, *Infect. Immun. 72*, 2123−2130.
67. McNeely, T. B., and Turco, S. J. (1990) Requirement of lipophosphoglycan for intracellular survival of *Leishmania donovani* within human monocytes, *J. Immunol. 144*, 2745−2750.
68. Beckman, J. S., and Koppenol, W. H. (1996) Nitric oxide, superoxide, and peroxynitrite: the good, the bad, and ugly, *Am. J. Physiol. 271*, C1424−C1437.
69. Ischiropoulos, H., Zhu, L., and Beckman, J. S. (1992) Peroxynitrite formation from macrophage-derived nitric oxide, *Arch. Biochem. Biophys. 298*, 446−451.
70. Albakri, Q. A., and Stuehr, D. J. (1996) Intracellular assembly of inducible NO synthase is limited by nitric oxide-mediated changes in heme insertion and availability, *J. Biol. Chem. 271*, 5414−5421.
71. Koike, E., Kobayashi, T., Mochitate, K., and Murakami, M. (1999) Effect of aging on nitric oxide production by rat alveolar macrophages, *Exp. Gerontol. 34*, 889−894.
72. Hughes, K., Antonsson, A., and Grundstrom, T. (1998) Calmodulin dependence of NFkappaB activation, *FEBS Lett. 441*, 132−136.
73. Jang, M. K., Goo, Y. H., Sohn, Y. C., Kim, Y. S., Lee, S. K., Kang, H., Cheong, J., and Lee, J. W. (2001) Ca^{2+}/calmodulin-dependent protein kinase IV stimulates nuclear factor-kappa B transactivation via phosphorylation of the p65 subunit, *J. Biol. Chem. 276*, 20005−20010.

BI060485P